Cell, Vol. 102, 797–808, September 15, 2000, Copyright ©2000 by Cell Press

Ciboulot Regulates Actin Assembly during *Drosophila* Brain Metamorphosis

Isabelle Boquet,* Rajaa Boujemaa,† Marie-France Carlier,† and Thomas Préat*‡
*Laboratoire Développement, Evolution, et Plasticité du Système Nerveux
Institut de Neurobiologie Alfred Fessard
CNRS
91190 Gif-sur-Yvette
France
†Laboratoire d'Enzymologie et Biochimie Structurale
CNRS
91190 Gif-sur-Yvette
France

Summary

A dynamic actin cytoskeleton is essential for the remodeling of cell shape during development, but the specific roles of many actin partners remain unclear. Here we characterize a novel actin binding protein, Ciboulot (Cib), which plays a major role in axonal growth during *Drosophila* brain metamorphosis. Loss of Cib function leads to axonal growth defects in the central brain, while overexpression of the gene during development leads to overgrown projections. The Cib protein displays strong sequence similarity to β-thymosins but has biochemical properties like profilin: the Cib-actin complex participates in actin filament assembly exclusively at the barbed end, and Cib enhances actin-based motility in vitro. Genetic experiments show that Cib and the *Drosophila* profilin protein Chickadee (Chic) cooperate in central brain metamorphosis.

Introduction

The metamorphosis of the *Drosophila* central nervous system is a complex developmental step. Most studies have focused on the metamorphosis of the ventral ganglia and have revealed three different cellular fates (reviewed by Truman, 1990). Many larva-specific neurons are definitively removed by programmed cell death, while most of the remaining cells withdraw their larval projections and extend new processes. Some neurons, specific to the adult stage, differentiate at metamorphosis.

In the adult brain protocerebrum, two central structures have been the focus of particular attention, the mushroom bodies (MB) and the central complex (CX). In the adult, the MB send their axons into the peduncle to terminate in one of three sets of lobes (α and β, α′ and β′, γ and spur) (Crittenden et al., 1998). MB are already present in a miniature state in the late embryo (Tettamanti et al., 1997; Armstrong et al., 1998) and are remodeled through larval and pupal development in a sequential manner (Technau and Heisenberg, 1982; Tettamanti et al., 1997; Lee et al., 1999). The CX, in contrast, is entirely built up during metamorphosis from immature neurons of the brain commissure (Hanesch, 1986; Truman et al., 1993; Renn et al., 1999). The mechanisms involved in the remodeling of the MB (Kraft et al., 1998) and CX during metamorphosis remain largely unknown.

During neuronal differentiation, actin-rich membrane structures called lamellipodia and filopodia are localized at the leading edge of the growth cones. These processes explore the extracellular environment to find appropriate targets. Much of the current understanding of growth cone motility is based on knowledge gained from actin filament dynamics in nonneuronal cell types, such as fibroblasts (reviewed by Stossel, 1993), or in cultured neurons (Bradke and Dotti, 1999), and recently actin-based motility has been reconstituted in vitro from a small set of pure proteins (Loisel et al., 1999). Directed motility of filopodia is mediated by the dynamic remodeling of the actin cytoskeleton in response to guidance signals (for reviews see Smith, 1988; Gallo and Letourneau, 1999; Korey and Van Vactor, 2000). During brain development, expression of several actin-interacting proteins is tightly correlated with neuronal differentiation (Roth et al., 1999). However, the nature and function of specific actin binding proteins involved in brain development remain poorly understood.

In *Drosophila*, several proteins have been implicated in the transmission of guidance signals toward the actin cytoskeleton during embryonic neuronal differentiation (for reviews see Lanier and Gertler, 2000; Lin and Greenberg, 2000). *chickadee* (*chic*) encodes the actin binding protein profilin, and *chic* mutations lead to various defects in actin-dependent processes such as intercellular cytoplasm transport during oogenesis (Cooley et al., 1992) or bristle malformation (Verheyen and Cooley, 1994). Recently, *chic* was shown to be required for the embryonic growth cone guidance of motoneurons (Wills et al., 1999). However, the Chic-actin interaction has yet to be analyzed at the biochemical level.

In a screen for adult central brain mutants, lines displaying central brain expression patterns (Simon et al., 1998) at the third instar larval stage were identified (Boquet et al., 2000). This work led to the recovery of six adult central brain mutants. Here we analyze one of the corresponding genes, *ciboulot* (*cib*), localized at band 4B on the X chromosome. Adult mutants deficient for *cib* display arrest in axonal growth in the CX, while overexpression of *cib* leads to overgrown MB projections. We show that *cib* encodes a protein with strong sequence similarities to β-thymosins. Like β-thymosin, Cib binds monomeric actin. However, unlike β-thymosin-actin, the Cib-actin complex participates in actin polymerization and is functionally similar to the profilin-actin complex. In addition, we show that *cib* and *chic* function together and that overexpressing Chic can compensate for the lack of Cib in adult brain development. These results provide novel evidence for the importance of actin assembly dynamics in neuronal differentiation and demonstrate the crucial role of actin binding proteins in adult brain formation.

‡To whom correspondence should be addressed (e-mail: preat@iaf.cnrs-gif.fr).

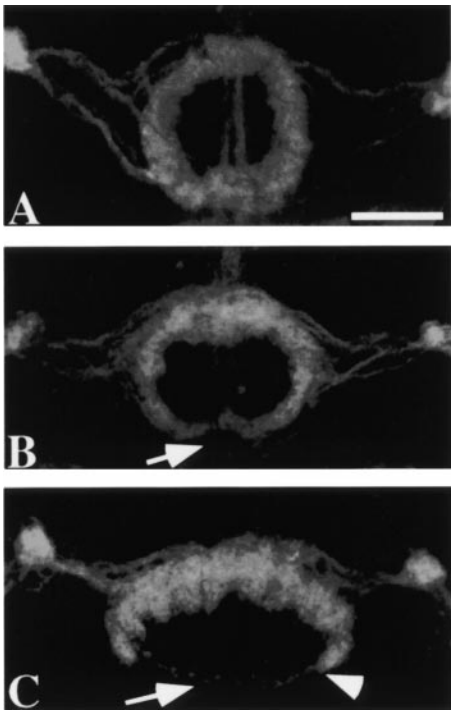

Figure 1. Confocal Analysis of the Central Brain Defect in the Adult Mutant *cib* Outlined with a Structural Marker of the Ellipsoid Body

(A) Whole-mount normal brain of *gal1625,UAScd8GFP/+* fly showing intact ellipsoid body.

(B and C) Whole-mount brain of *cib^{E10}/Y; gal1625,UAScd8GFP/+*: the ellipsoid body is ventrally opened with various expressivity (arrows) and in some cases fewer fibers are present at the arrest point (arrowhead in [C]). Scale bar, 50 μm.

Results

cib Ellipsoid Body Neurons Fail to Achieve Complete Growth

The CX is located at the adult interhemispheric junction and consists of a neuropilic structure composed of ~20,000 neurons divided into four substructures, organized rostrally to caudally: the ellipsoid body (EB), the fan-shaped body (FB) with its pair of nodulli, and the protocerebral bridge (Hanesch et al., 1989). In *cib* mutants, the ellipsoid body is ventrally opened or even more severely disorganized (Boquet et al., 2000). Several *cib* mutant alleles are available, including *cib^{P}*, *cib^{E10}*, and *Df(1) A113*, a large deficiency removing several genes. *cib^{P}*, *cib^{E10}* flies are homozygous viable; *Df(1) A113* is lethal, but *cib^{P}/Df(1) A113* are viable. *cib^{P}*, *cib^{E10}* and *cib^{P}/Df(1) A113* flies display similar central brain defects (Boquet et al., 2000), suggesting that *cib^{P}* corresponds to a null mutation and that *cib* is not an essential gene, as confirmed by Western blot analysis (see below).

The central brain *cib* defect was further characterized using EB-specific enhancer trap lines as structural markers. The *gal1625* line displays an expression pattern that is restricted to some ring neurons in the adult EB (Figure 1A). At the onset of normal pupal formation, the EB precursor appears as a flat neuropilic structure, consisting of dorsal fibers of the future EB. During metamorphosis, the putative EB neuropil elongates downward to form the characteristic ring-like structure (K. Ito, personal communication). In a *cib* context, the EB shows axonal growth arrest with various expressivity (Figures 1B and 1C).

cib Encodes a 14.4 kDa Protein that Consists of Three β-Thymosin Repeats

Cloning of *cib* was initiated from the P element insertion allele, *cib^{P}*. Genomic DNA flanking the 5′ end of the P element was recovered from adult DNA by PCR rescue. The amplified fragment of 0.3 kb was sequenced. The contig EG0007 (European *Drosophila* Genome Project) was shown to include the *cib* genomic fragment, which corresponds to the predicted gene EG0007-11 located between *brainiac* and *fasciclinII* (Figure 2A). Two larval and/or pupal cDNA clones are available (Berkeley *Drosophila* Genome Project), LP07643 and LP05275. These two cDNAs are derived from alternatively spliced RNAs and differ in the nature of the first noncoding exon (Figure 2A). The common open reading frame, which starts at the first residue of exon 3 and ends just before the end of exon 5, encodes a 129 amino acid protein (M_r 14.4 kDa).

The sequence of Cib (Figure 2B) exhibits three similar domains D1, D2, and D3. D1 and D2 display 47% sequence identity, D1 and D3, 50%, and D2 and D3, 67%. D3 contains a 10 amino acid sequence, KLKHTETNEK, which represents an actin binding motif very similar to that found in β-thymosins (Nachmias, 1993), a family of small (5 kDa) actin binding proteins present in vertebrates (Erickson-Viitanen et al., 1983) and sea urchins. A motif similar to KLKHTETNEK is also found in other actin binding proteins, including actobindin, a 9 kDa actin binding protein found in *Acanthamoeba castellanii* (Vandekerckhove et al., 1990; Bubb and Korn, 1995), as well as verprolin in *Saccharomyces cerevisiae* (Vaduva et al., 1997, 1999), its homolog WIP (WASP-interacting protein), and proteins of the WASP family in mammalian cells (Ramesh et al., 1997). A *C. elegans* Cib homolog was identified, which exhibits four similar domains. The overall sequence comparison between the Cib D3 domain and these proteins is shown in Figure 2B.

The D2 and D3 Cib domains display an overall sequence identity with rat thymosin β4 (Tβ4) of 54% and 65%, respectively (Hannappel et al., 1982). All β-thymosins bind G-actin specifically in a 1:1 molar ratio (Safer and Chowrashi, 1997) with an affinity in the 10^6 M^{-1} range and behave as passive G-actin sequestering proteins that create a pool of unassembled monomeric actin (for reviews see Yu et al., 1993; Carlier and Pantaloni, 1994). The strong sequence identity between Cib and thymosin β4 suggests that it may interact with actin. The function of Cib in brain development was further addressed in biochemical and genetic experiments.

The Cib Protein Is Strongly Expressed during Metamorphosis

Polyclonal antibodies were raised against a GST-Cib fusion protein expressed in *E. coli*. These antibodies detected by Western blot a 14 kDa protein in third instar larvae, 24-hr-old pupae, and adults (Figure 3A). The level of expression of Cib in pupae was significantly increased, suggesting that *cib* may be important during metamorphosis. The Cib protein was detected in wild-type embryos (Figure 3A) but not in *cib^{E10}/+* embryos laid by mutant *cib^{E10}/cib^{E10}* females, indicating that the embryonic product corresponds exclusively to maternal protein accumulated during oogenesis (Figure 3A). The

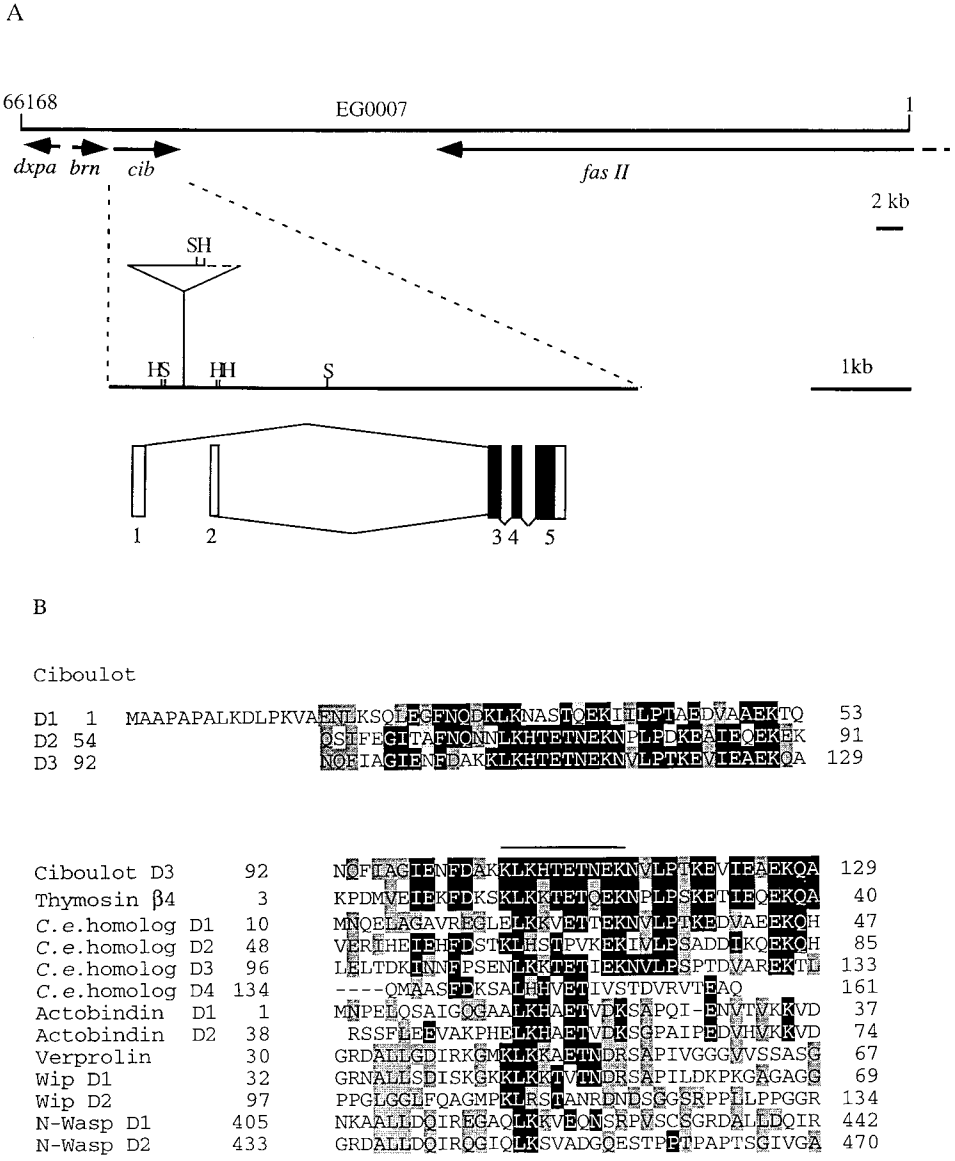

Figure 2. Organization of the *cib* Locus

(A) Part of genomic DNA of the EG0007 contig, carrying *cib* and the insertion site of the P element are shown. Two mRNAs are represented that differ in their first exon. These two mRNAs give rise to the same conceptual protein (coding regions are in black). Restriction sites used for gene analysis were HpaII (H) and Sau3A1 (S).

(B) Alignment of three Cib domains with themselves and alignment of Cib D3 domain with several actin binding proteins and with the four domains of *C. elegans* homolog (*C. elegans* putative protein F08F1.8; ID, AAB71308.1). The conserved motif of 10 amino acids is overlined.

protein was detected in the head of adult *CS* and in phenotypic revertant cib^{E5} flies, whereas no product was found in the head of adult cib^{P} or cib^{E10} flies (Figure 3B), both of which display a mutant ellipsoid body. The temporal expression pattern of Cib thus confirms the conclusions of the genetic analysis and supports the idea that *cib* is required for correct central nervous system development during metamorphosis.

cib Is Expressed in Central Brain Structures

The polyclonal anti-Cib serum failed to detect the protein on fixed tissues. Therefore, the expression pattern of *cib* was analyzed by in situ hybridization and with the *P(Gal4)* element inserted in the 5′ region of the gene. In situ hybridization revealed the presence of *cib* mRNA in the brain of third instar larvae (data not shown) and of 60-hr-old pupae (Figure 4A). Strong expression was detected in the pars intercerebrallis and in four clusters of cell bodies in each hemisphere, which most likely belong to the four clusters of MB Kenyon cells (Ito et al., 1997). No expression was detected in cib^{E10} mutants (data not shown).

Brains of $cib^{P}/+$; *UASmCD8::GFP* third instar larvae (data not shown), 60 hr pupae (Figures 4B and 4C), and adults (data not shown) were dissected, which showed strong GFP expression in the MB at all stages (the absence of any defect in *cib* MB is dealt with in the Discussion section). Weaker expression was detected in the ellipsoid body at pupal stages (Figure 4C), suggesting

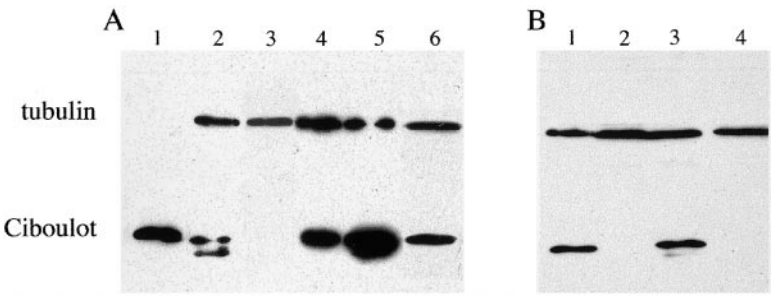

Figure 3. Western Blot Analysis of Cib Expression

Fifty micrograms of total protein extracts were loaded per lane. Blots were probed with polyclonal antibody raised against the fusion protein GST-Cib.

(A) Developmental analysis of Cib expression in wild type (except lane 3). Lane 1, 200 ng of bacterially expressed Cib (control). Lane 2, embryos. The lower band most likely corresponds to partial Cib degradation (see Experimental Procedures). Lane 3, embryos laid by cib^{E10} females mated with *CS* males. Lane 4, third instar larvae. Lane 5, 24-hr-old pupae. Lane 6, adults.

(B) Analysis of Cib expression in mutants. Adult head protein extracts. Lane 1, *CS*. Lane 2, cib^{P}. Lane 3, phenotypic revertant excision cib^{E5}. Lane 4, mutant excision cib^{E10}.

that autonomous expression of the gene in the EB is required for proper formation of this structure. No expression was detected in embryos (data not shown), confirming the Western blot analysis.

Cib Forms a 1:1 Complex with Monomeric Actin

The interaction of Cib with G-actin was studied by analytical ultracentrifugation. Sedimentation velocity measurements showed that the sedimentation coefficient of G-actin was increased from 3.2 S to 3.6 S upon addition of Cib. Chemical cross-linking of Cib to G-actin using the zero-length cross-linker EDC at different Cib:actin molar ratios yielded a single covalently cross-linked polypeptide (Figure 5A). These results indicate that Cib binds G-actin in a 1:1 molar ratio. Cib was never found to be associated with F-actin in sedimentation assays (data not shown). Hence, Cib appears to bind G-actin specifically.

The Cib-G-Actin Complex Participates in Filament Assembly at the Barbed Ends, Not at the Pointed Ends, in a Manner Functionally Similar to Profilin-G-Actin

The effect of Cib on actin assembly was investigated in steady-state and kinetic measurements. The hydrolysis of ATP associated with actin polymerization makes actin filaments nonequilibrium polymers with different critical concentrations at the barbed and pointed ends. When both ends of the filament are free, the steady-state G-actin concentration (0.12 μM under physiological conditions) is slightly higher than the critical concentration at the barbed ends, and filaments treadmill, i.e., barbed end growth balances pointed end shortening. When barbed ends are capped, for example by gelsolin, monomer association to and dissociation from the barbed ends is abolished, and the measured steady-state G-actin concentration equals the critical concentration at the pointed ends (0.6 μM under physiological conditions).

In the presence of gelsolin, Cib induced a shift in the critical concentration plots, indicating that the Cib-G-actin complex does not participate in polymerization at the pointed end (Figure 5B). Accordingly, addition of Cib to gelsolin-capped filaments caused depolymerization of F-actin in a linear fashion with the amount of Cib added (Figure 5C). The two sets of data are consistent with an equilibrium dissociation constant of 2.5 $\pm$ 1 μM for the Cib-G-actin complex.

When barbed ends were not capped, the results were strikingly different. Cib no longer behaved as a G-actin sequestering protein causing F-actin depolymerization. Rather, a slight increase in the amount of F-actin at steady state was observed in the presence of Cib (Figures 5B and 5C). The Cib-G-actin complex thus behaves as the profilin-G-actin complex as it participates in actin assembly at the barbed end (Pollard and Cooper, 1984; Pring et al., 1992; Pantaloni and Carlier, 1993).

The different effects of Cib on actin assembly at the two ends were confirmed in kinetic measurements of barbed and pointed end growth from G-actin subunits (Figure 5D). Filament elongation at the pointed end was inhibited by Cib in a saturation-dependent fashion consistent with Cib forming a complex with G-actin that was not able to associate with pointed ends. In contrast, a very small decrease in the rate of barbed end growth was observed when G-actin was saturated by Cib. At very high, nonphysiological concentrations of Cib (100 μM), partial inhibition of barbed end growth was observed, possibly due to low-affinity barbed end capping (data not shown).

Finally, Cib, like profilin (Pollard and Cooper, 1984), inhibited spontaneous polymerization of G-actin and increased the lag phase due to filament nucleation (Figure 5E). However, active polymerization took place subsequent to fragmentation of filaments by pipetting, thus confirming that nucleation but not barbed end growth was inhibited by Cib. The effect of Cib on actin assembly is summarized in Figure 5F.

To verify that the properties of bacterially expressed Cib were also observed with the endogenous *Drosophila* protein, a partial purification (about 50-fold) of Cib from wild-type (*CS*) pupae was carried out (see Experimental Procedures). A control batch of mutant *cib* pupae was treated identically. The Cib protein represented about 4% of the total protein in the semipurified *CS* extract and was absent in the mutant extract (Figure 5G). Comparative measurements of barbed and pointed end growth rates in the presence of identical amounts of the two extracts revealed that the presence of Cib in the wild-type extract caused inhibition of pointed end but not of barbed end growth (Figure 5G). The wild-type extract but not the mutant extract caused an inhibition of spontaneous polymerization, attributed to Cib (Figure

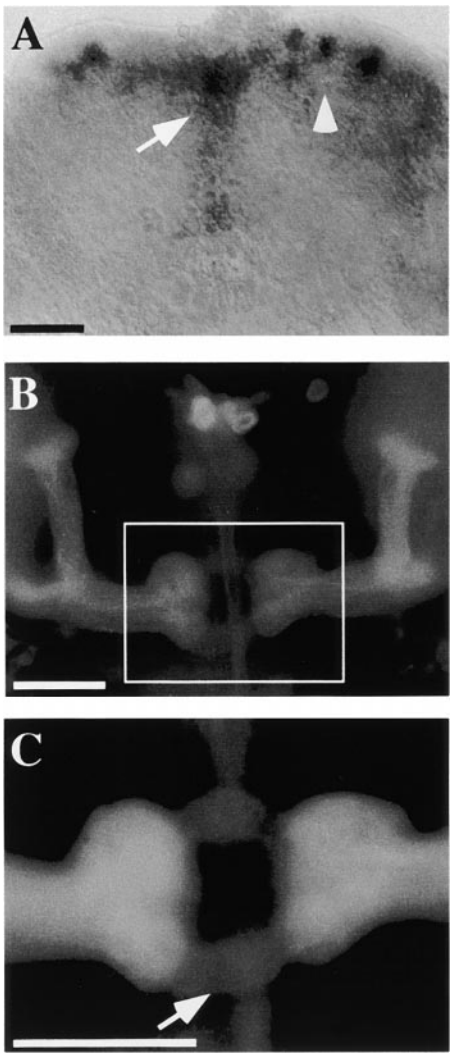

Figure 4. Brain Expression of *cib*

(A) In situ hybridization to 60-hr-old pupae. *cib* mRNA was observed in the pars intercerebrallis (arrow) and in four clusters of cell bodies in each hemisphere (arrowhead), corresponding to MB Kenyon cells. (B) Whole-mount brain of 60-hr-old cib^{P}/+;*UAScd8GFP* pupae. Expression was observed in the pars intercerebralis and in the MB. (C) Expression is detected at a lower level in the EB during metamorphosis (arrow). Scale bar, 50 μm.

5H). Although the complete purification of Cib was hampered by extensive proteolytic degradation—probably reflecting the fact that Cib, like thymosin β4, may not be highly structured—the present results indicate that the endogenous *Drosophila* protein exhibits the same function as the bacterially expressed Cib protein.

Cib Can Replace Profilin in Enhancing Actin-Based Motility of *Listeria monocytogenes*

Profilin enhances actin-based motility (Loisel et al., 1999) due to the ability of the profilin-actin complex to support exclusive barbed end growth. Profilin thus increases the processivity of treadmilling and the rate of barbed end growth in the presence of actin-depolymerizing factor (Didry et al., 1998). The resulting effect of profilin in actin-based motility is readily measured in the motility assay of *Listeria monocytogenes* reconstituted from pure proteins (Loisel et al., 1999). *Listeria* moves slowly (0.3 ± 0.25 μm/min) in the profilin-free medium and 3- to 4-fold faster in the presence of profilin (Table 1). Cib showed the same effect as profilin on actin-based motility, consistent with the functional similarity of the two proteins. Actobindin, the amoeba G-actin binding protein, which shows sequence homology with Cib (Figure 2B) and which, like Cib and profilin, does not inhibit barbed end growth (Bubb and Korn, 1995), also enhanced actin-based motility (Table 1). In contrast, thymosin β4 did not increase the rate of *Listeria* propulsion. This result is expected since Tβ4 passively sequesters G-actin and the Tβ4-actin complex does not participate in actin filament dynamics. At very high Tβ4 concentrations, complete depolymerization of the F-actin in the medium arrested movement as a result of the disruption of the dynamic filament system undergoing treadmilling, which is the support of steady movement.

cib Interacts Genetically with the Profilin-Encoding Gene *chic*

The functional homology between Cib and profilin was tested in vivo by examining the genetic interaction between *cib* and *chic*. In $chic^{221}$/+ flies, which presumably have only half of the profilin found in normal flies, there were no structural brain abnormalities (data not shown). Similarly, heterozygote cib^{P}/+ females displayed no abnormal brain phenotype in paraffin section (Boquet et al., 2000). However, cib^{P}/+; $chic^{221}$/+ doubly heterozygote females displayed a *cib*-like phenotype, with a partially split fan-shaped body (Figure 6D), a ventrally opened ellipsoid body (Figure 6E), and normal MB (Figure 6F). Thus, the interaction between *cib* and *chic* is not additive but synergistic.

Reducing by half the Chic activity in *cib* mutants exacerbated the phenotype normally associated with *cib*: cib^{P}/Y; $chic^{221}$/+ males displayed a fan-shaped body split in the middle (Figure 6G), an ellipsoid body strongly disturbed (Figure 6H), similar to that observed in *trio* mutants (Awasaki et al., 2000), and disorganized MB medial lobes that rarely reached their normal position (Figure 6I). These results show that *chic* is involved in adult brain formation and, moreover, support the view that Cib acts synergistically with Chic in vivo. Furthermore, cib^{P}/Y; $chic^{221}$/+ males displayed other phenotypes that can be related to impaired actin-dependent developmental processes (Verheyen and Cooley, 1994), including sterility and a thoracic bristle defect with shorter and forked ends (data not shown), possibly resulting from the defective formation of the peripheral nervous system. Chic rather than Cib is the principal source of profilin function during gametogenesis since *chic* but not *cib* mutants are sterile. However, the reduced profilin in $chic^{221}$/+ flies is partially compensated by Cib^{+}, allowing fertility (in other words, $chic^{221}$ is recessive in an otherwise wild-type background but semidominant in a *cib* background).

We next wondered if the defects induced by the lack of Cib could be rescued by increasing the supply of Chic profilin. We did this by introducing a $chic^{+}$ duplication into a *cib* mutant. Two duplications were available, *Dp(2;2)C619* (26A;28E), which was shown to rescue embryonic *chic* axonal phenotype (Wills et al., 1999), and *Dp(2;2)Cam2* (23D01-02;26C01-02). These two duplications overlap over 26A;26C01-02, a small region that

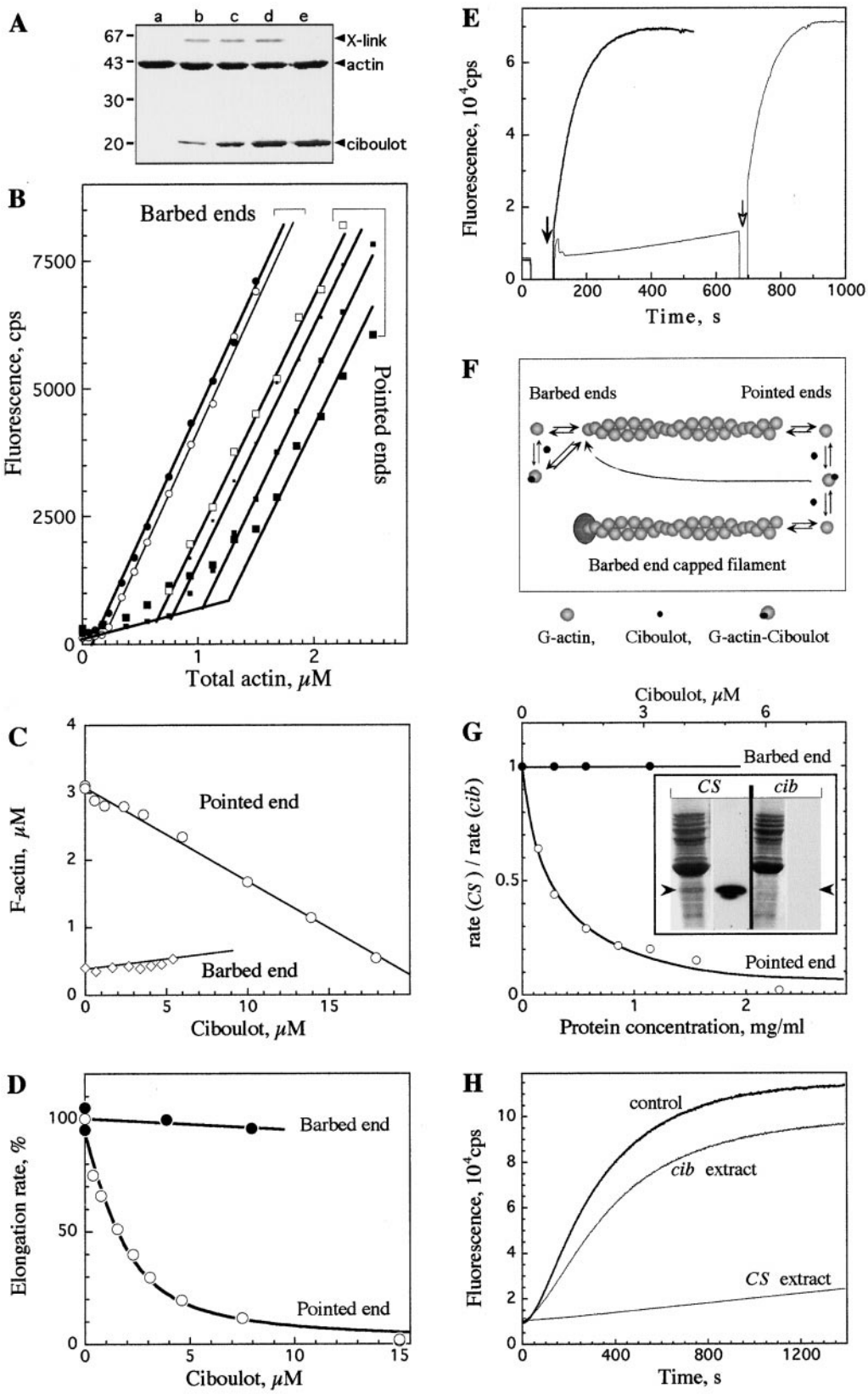

Figure 5. Cib Binds G-actin in a 1:1 Complex that Participates in Actin Polymerization at the Barbed Ends, Not at the Pointed Ends of Actin Filaments

(A) Covalent EDC cross-linking of the Cib-actin complex. G-actin (5 μM) was EDC cross-linked in the absence (a) or in the presence of 5 μM (b), 10 μM (c), or 20 μM (d) Cib (e). Control lane without covalent cross-link of the Cib-actin complex. Molecular weight scale is shown in kDa.

Table 1. Compared Effects of Profilin, Ciboulot, Actobindin, and Thymosin β4 on Actin-Based Motility of *Listeria*

Added Protein	Concentration (μM)	Average Bacterial Rate (μm · min^{-1})	Number of Measurements
None	—	0.32 ± 0.02	10
Profilin	2.5	1.27 ± 0.2	11
Ciboulot	0.5	0.93 ± 0.2	12
	2.0	1.23 ± 0.2	12
	4.0	1.00 ± 0.3	16
	13.7	0.96 ± 0.2	13
Actobindin	0.25	0.60 ± 0.1	11
	0.5	1.30 ± 0.1	12
	1.0	0.97 ± 0.1	12
	2.5	<0.1	12
Thymosin β4	2.5	0.34 ± 0.03	13
	5.0	0.35 ± 0.06	12
	10.0	No actin assembly at bacterial surface	—

spans the *chic*$^{+}$ locus (26A09–26B01). The phenotype of *cib*^{E10}*/Y; Dp(2;2),chic*$^{+}$*/+* was compared to that of *cib*^{E10}*/Y; CyO/+* siblings, the latter genotype being used as a control of *cib* phenotype in the appropriate genetic background. Interestingly, *cib*^{E10}*/Y; Dp(2;2),chic*$^{+}$*/+* individuals displayed a normal brain (Figure 6K), whereas *cib*^{E10}*/Y; CyO/+* adults displayed a strong *cib* phenotype (Figure 6J). The full rescue of *cib* defects by increasing the ubiquitous Chic supply confirms the profilin-like function of Cib in vivo.

A genetic interaction between *chic* and the tyrosine kinase encoding gene *Abl* has been previously described (Wills et al., 1999). We observed that *cib*^{P}*/Y;Abl*^{04674}*/+* individuals displayed a stronger phenotype than their *cib*^{P}*/Y;TM3/+* siblings (data not shown). Thus, *cib* and *chic* interact similarly with *Abl*, which supports the assumption that they both are active in the same pathway.

Overexpression of Cib during Development Leads to Overgrown MB Projections

As a decreased axonal growth is observed in the absence of Cib, we wondered whether overexpressing the actin binding protein would lead to increased axonal growth. An inducible *hs-cib*$^{+}$ transgene was made that allowed overexpression of Cib during development. The effect was assessed at the level of the MB, as they consist of parallel neuron bundles, the ends of which can be easily traced. MB β lobes overgrew and crossed the midline when Cib was overexpressed (Figure 7). Identical results were obtained when Cib expression was driven specifically in the MB using a *UAS-cib*$^{+}$ construction and MB-expressed *PGal4* lines (data not shown).

Discussion

We have identified a novel actin binding protein, Cib, that plays an important role in the development of the central nervous system of *Drosophila*. The function of Cib has been revealed using a combination of genetic studies, in vitro biochemical experiments, and actin-based motility assays. Cib has the same regulatory function as profilin in actin assembly, although it shares no sequence similarity with profilin. We have shown that

(B) Cib shifts the critical concentration plots for actin assembly at pointed ends. Steady-state fluorescence measurements of F-actin polymerization in the absence (circles) or presence (squares) of gelsolin (gelsolin:actin ratio 1:300) without (open symbols) and with (closed symbols) Cib at the following concentrations (in μM): 0.66 (small squares), 1.68 (middle squares), 3.34 (largest squares), and 1.68 (closed circles).

(C) Cib depolymerizes F-actin only when barbed ends are capped. Cib was added at the indicated concentrations to a solution of standard F-actin at 0.5 μM (free barbed ends, diamonds) or of gelsolin-capped F-actin at 3.6 μM (circles). The amount of F-actin at steady state was derived from fluorescence measurement of pyrenyl-F-actin.

(D) Cib-actin complex participates in filament growth at the barbed end, not at the pointed end. The rate of ATP-G-actin association to the barbed ends (closed circles, spectrin-actin seeds) and to the pointed ends (open circles, gelsolin-actin seeds) was measured.

(E) Cib inhibits spontaneous formation of F-actin by interfering with actin nucleation. MgATP-G-actin (10 μM, 10% pyrenyl-labeled) was polymerized in the absence (thick line) or in the presence of 5 μM of Cib (thin line). Polymerization was started by addition of 0.1 M KCl and 1 mM $MgCl_2$ (filled arrow). At time indicated by the empty arrow, the solution was sheared by pipetting, leading to filament fragmentation followed by elongation.

(F) Model for the interaction of Cib with G-actin. Cib makes a 1:1 complex with G-actin. Cib-actin complex productively associates with barbed ends in a profilin-like fashion, while association with pointed ends is inhibited, making Cib a G-actin sequestering protein when barbed ends are capped.

(G) Effect of semipurified *Drosophila* Cib on barbed and pointed end growth. Semipurified extracts of wild-type (*CS*) and *cib* pupae (see Experimental Procedures) were assayed as for (D). The rates of filament elongation were measured at identical total protein concentration. The ratio of the rates measured for *CS* and *cib* at the barbed end (closed circles) and at the pointed end (open circles) is plotted versus the total concentration of protein added (lower scale) or the calculated concentration of Cib present in the wild type extract (upper scale). Inset, Coomassie blue staining SDS gel patterns and Western blotting of the semipurified extracts showing the presence (arrow) or absence of Cib.

(H) Effect of the semipurified extracts on spontaneous polymerization of actin. The experiment was conducted as for (E), except that the actin concentration was 7.5 μM. The amount of total protein added was 1.1 mg/ml, corresponding to about 3 μM Cib in the *CS* sample (no extract was added for the control curve).

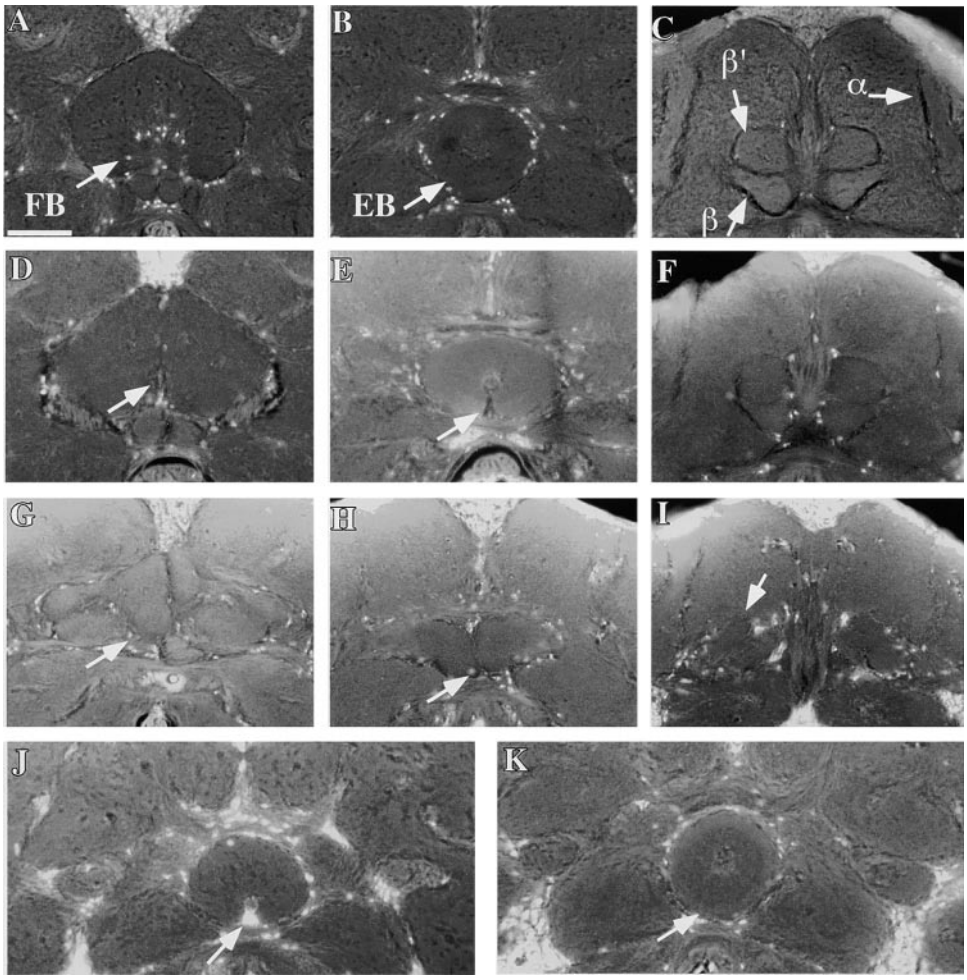

Figure 6. Synergistic Interaction of *cib* and *chic* during Adult Central Brain Differentiation

Frontal paraffin sections of adult brains at the level of the CX in *CS* flies (A–C), $cib^{P}/+$; $chic^{221}/+$ flies (D–F), and cib^{P}/Y; $chic^{221}/+$ flies (G–I). Natural fluorescence allows detection of cellular bodies in yellow and neuropil in green.

(A) The fan-shaped body (FB) displays the characteristic fig-like shape in *CS* flies (arrow).

(B) The ellipsoid body (EB) appears ring-like (arrow) in *CS* flies.

(C) The MB appear normal with medial lobes stopping at the midline.

(D) The FB is split in two along the midline in 10% of $cib^{P}/+$; $chic^{221}/+$ flies.

(E) The EB is ventrally opened in all $cib^{P}/+$; $chic^{221}/+$ flies. This phenotype is similar to that displayed by *cib* individuals (Boquet et al., 2000).

(F) The MB appear wild type.

(G) The FB is split in two or more pieces in all cib^{P}/Y; $chic^{221}/+$ flies (arrow).

(H) The EB is flat in all cib^{P}/Y; $chic^{221}/+$ flies and very often split in two along the midline (arrow).

(I) Medial lobes of the MB do not reach their normal position in cib^{P}/Y; $chic^{221}/+$ (arrow).

(J) The EB is flat in all cib^{E10}/Y; *CyO*/+ individuals, which carry a genetic background identical to their cib^{E10}/Y; *DpC619*,$chic^{+}/+$ siblings.

(K) The EB appears normal in cib^{E10}/Y; *DpC619*,$chic^{+}/+$ individuals. Scale bar, 50 μm.

both Cib and the *Drosophila* profilin Chic are required for the postembryonic development of central brain structures, and that *cib* mutant defect can be rescued by overexpressing Chic. Our data support the idea that the dynamic regulation of actin assembly is a key factor controlling axonal outgrowth during the fast differentiation events occurring in the central brain at metamorphosis.

cib Encodes a G-actin Binding Protein that Shows Strong Sequence Similarity to β-Thymosins and Functional Homology to Profilin

The 129 amino acids Cib protein harbors three similar domains, each of which contains an actin binding motif strongly similar to the sequence KLKKTETNEK, first identified in β-thymosins and conserved in a number of actin binding proteins (Figure 2B). However, Cib behaves in a manner functionally similar to profilin (Pollard and Cooper, 1984; Pring et al., 1992; Pantaloni and Carlier, 1993) since it sequesters G-actin when barbed ends are capped, but unlike thymosin β4, it actively shuttles actin subunits to feed the growth of free barbed ends. The Cib-G-actin complex even appears to polymerize better than G-actin itself. The fact that Cib supports unidirectional barbed end growth of actin filaments lead us to predict that its biological function, like that of profilin (Carlier et al., 1997; Didry et al., 1998), is to enhance the treadmilling of actin filaments in the pres-

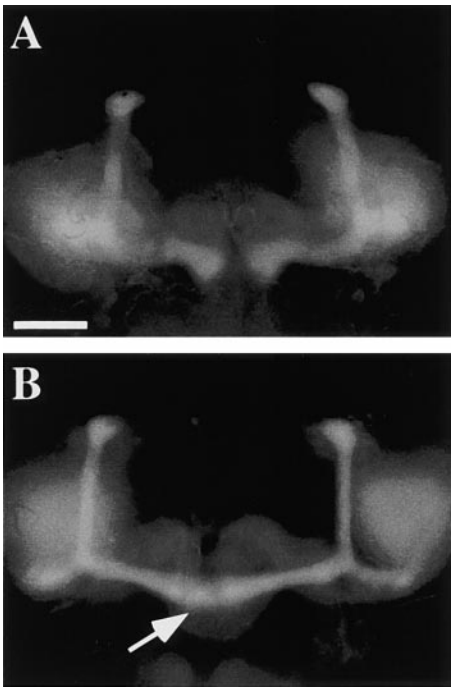

Figure 7. Overexpression of Cib Leads to Overgrown Mushroom Bodies, as Revealed by a *gal623* Marker

In toto preparation of adult brains.

(A) Brain of *gal623,UAScd8GFP/+* control flies which have undergone thermic shocks during development, where medial lobes of the MB stop at the midline.

(B) In *gal623,UAScd8GFP/+; hs-cib*$^{+}$*/+* flies following heat shock treatment during development, a β lobes fusion can be observed (arrow). Scale bar, 50 μm.

ence of cofilin and accelerate actin-based motile processes, such as those thought to be involved in directional axonal growth. In support of this view, Cib was able to replace profilin in increasing the rate of actin-based propulsion of *Listeria* in a motility medium reconstituted from pure proteins, and the *cib* central brain defect was fully rescued by increasing the Chic supply.

It is likely, given its effect on actin polymerization (Bubb and Korn, 1995) and on actin-based motility (present work) that actobindin has a similar function as Cib. More detailed biochemical studies of actobindin are underway to address this issue. More generally, a sequence close to the KLKHTETNEK motif is found in actin binding proteins, including actobindin in *A. castellanii*, verprolin in *S. cerevisiae* and its mammalian homolog WASP-interacting-protein (WIP), and the C-terminal domain of proteins of the WASP/Scar family that act as connectors between the signaling pathways and actin polymerization (Carlier et al., 1999; Machesky and Insall, 1999). Several features define them as a novel protein family that includes Cib (Bubb and Korn, 1995; Egile et al., 1999; this work): first, the consensus motif is imperfectly repeated (except in verprolin); second, several of these proteins bind G-actin with an affinity in the 10^6 M^{-1} range in essentially a 1:1 molar ratio (although weak binding of a second G-actin molecule to actobindin has been reported [Bubb et al., 1991]); third, these proteins inhibit nucleation and sequester G-actin when barbed ends are capped; fourth, they create a pool of sequestered actin in the cell medium, where the pointed critical concentration of G-actin is established by capping proteins, and promote actin assembly at barbed ends created in response to signaling.

In conclusion, the consensus sequence of 10 amino acids may define a novel class of actin binding proteins that share functional similarity with profilin and are important players in morphogenetic or developmental actin-based processes. Although β-thymosins appear to be bona fide members of this family, their complex with actin uniquely fails to participate in barbed end growth. Inspection of the sequences indicates that in thymosin β4, the amino acid residues E8 and K11, which are known to be important for the sequestering function (Van Troys et al., 1996), are generally replaced by noncharged residues in Cib and other members of this class (Figure 2B).

Sequence comparison indicated that Cib is the only *Drosophila* protein showing strong similarity to β-thymosins, as is its *C. elegans* homolog. We suggest that all proteins from this class had a profilin-like function early in evolution and that the sequestering effect displayed by vertebrate β-thymosins was acquired later. Further genetic and biochemical studies will have to be carried out to understand the structure–function relationship in all these proteins.

cib Is Expressed in Postembryonic Brain and Functions in Synergy with *chic* to Control Axonal Growth

The Cib product present in embryos results from the persistence of protein accumulated during oogenesis, as the gene is not expressed during embryonic development. This maternal protein is not necessary for embryo survival. *cib* is expressed postembryonically and its expression, like that of *chic* (Verheyen and Cooley, 1994), increases during metamorphosis, suggesting a crucial role for these two genes in axonal outgrowth.

In *cib* mutants, EB ring neurons stop growing before reaching the midline ventrally, presumably because of insufficient actin assembly. Similarly, axonal growth arrest of motoneurons of the neuromuscular junction is observed in *chic* mutants (Wills et al., 1999). Synergistic effects of Cib and Chic central brain development indicate that these two proteins function as partners, in particular when rapid actin assembly is required for CX differentiation.

Although *cib* is expressed in MB, *cib* mutants show no strong MB defect. This could be due to the fact that the differentiation of adult MB neurons could follow pioneer projections elaborated during embryogenesis—and therefore would be able to differentiate more slowly in the absence of Cib because they are guided—while CX neurons differentiate rapidly at metamorphosis. Interestingly, in *cib* mutants with reduced Chic profilin, the MB medial lobes are disorganized, showing that the two genes also cooperate during MB development. Conversely, when Cib is overexpressed, neuron overgrowth occurs in the β lobes of the MB, as if the rate of actin assembly was too high. These results suggest that the concentration of Cib is finely regulated to ensure optimum axonal growth by mechanisms that remain to be elucidated. For example, a negative posttranscriptional regulation might occur in the MB that could involve the noncoding exons, absent in the two constructs used to overexpress *cib*.

cib is also expressed in the adult head and in particular

in the MB, the olfactory memory center, suggesting that it may play a role in neuronal plasticity. Indeed, dynamic actin assembly has been shown to correlate with the reorganization of synaptic connections in the mature nervous system (Matus, 1999).

This work demonstrates the importance of the regulation of actin assembly in neuronal outgrowth during brain formation, linking molecular events to changes at the cellular and the organ level. We anticipate that Cib will cooperate in vivo not only with Chic but also with other putative *Drosophila* components of the motile machinery, such as the G-actin sequestering protein Act-up (Benlali et al., 2000) and the signaling pathway toward actin cytoskeleton.

Experimental Procedures

Drosophila Stocks

Drosophila were maintained on a 12:12 dark/light cycle on standard cornmeal-yeast agar medium at 25°C and 50% relative humidity. The wild-type strain was *Canton-Special* (*CS*). The *Dp(2;2)C619* (spanning 26A;28E), *Dp(2;2)Cam2,sp*^{1} (spanning 23D01-02;26C01-02), *UAS-mCD8::GFP*, *Abl*^{04674}, *ry*^{506}*/TM3*, and the *chic*^{221}, *cn/CyO* stocks were all provided by the Bloomington stock center. *chic*^{221} is a lethal allele (Verheyen and Cooley, 1994). The *w*^{1118} *cib*^{P} allele was induced by *P(Gal4)* mutagenesis (Boquet et al., 2000); *w*^{1118} *cib*^{E5} and *w*^{1118} *cib*^{E10} alleles were obtained by excision of the P element of *cib*^{P} flies (Boquet et al., 2000). Southern analysis showed that *cib*^{E10} does not carry a genomic deficiency but rather retains some P sequences inserted in the *cib* gene (data not shown). All *cib* chromosomes carry the *w*^{1118} mutation, even when omitted in the text. In all experiments, the *cib*^{P} allele was used freshly outcrossed to a *w*^{1118} stock carrying a *CS* background, as in Boquet et al. (2000). Lines *gal1625*, *gal623*, and *gal4350* were generated in our laboratory after *P(Gal4)* enhancer trap mutagenesis and recombined with *UAS-mCD8::GFP*.

Molecular Biology

Genomic DNA adjacent to the P element insertion site was isolated by PCR rescue. Genomic DNA was isolated from *w*^{1118} *cib*^{P} flies and dialyzed through a microdialysis membrane. DNA was digested by HpaII and ligated at diluted concentration (20 ng/μl). Oligonucleotides of the 5′ end of PGawB element were used for PCR rescue. A 0.3 kb fragment was recovered and used as a probe for Southern blot analysis of the adjacent genomic DNA of several alleles of *cib* mutants. This 0.3 kb fragment was sequenced.

The *cib* open reading frame was cloned in fusion with the GST in NcoI–HindIII sites of the expression vector PGex2T* (Pharmacia). The entire open reading frame of the LP07643 cDNA clone (minus first methionin codon) was amplified by PCR and cloned in PCR 2-1 (Invitrogen) as an intermediary step. *hs-cib*$^{+}$ and *UAS-cib*$^{+}$ constructions were obtained by cloning the entire open reading frame of LP07643 in BglII–XbaI sites of pUAS (Schneuwly et al., 1987) and pCasper-hs (Brand and Perrimon, 1993) plasmids. The cDNA insert in LP07643 was amplified by PCR using to oligonucleotides carrying adaptors including either BglII or XbaI cutting sites and was cloned in PCR2-1 as an intermediate step.

The sequence of all PCR-amplified fragments was checked following cloning.

Proteins

Actin was purified from rabbit muscle, isolated as a CaATP-G-actin by sephadex G 200 gel filtration in G buffer (5 mM Tris-Cl, pH 7.8; 0.2 mM ATP; 0.1 mM DTT; 0.01% NaN_3), and pyrenyl labeled (Pantaloni and Carlier, 1993). Gelsolin was a kind gift of Dr. Yukio Doi (University of Kyoto, Japan), and actobindin purified from *Acanthamoeba castellanii* was a kind gift of Dr. Michael Bubb (University of Florida, Gainsville). Spectrin-actin seeds (Casella et al., 1995), thymosin β4 and profilin (Pantaloni and Carlier, 1993), actin-depolymerizing factor (Ressad et al., 1998), Arp2/3 complex (Egile et al., 1999), and human His-tagged VASP (Laurent et al., 1999) were prepared as described.

The fusion protein GST-Cib cloned in the expression vector p-GEX2T* (Pharmacia) was induced in *E. coli* strain *BL21* and purified as in Smith and Johnson (1988). The Cib protein was then cleaved with thrombin, dialyzed against a 10 mM Tris-chloride solution (pH 7.5), and concentrated through centricon membrane of 3 kDa holes (Millipore). Protein concentration was determined using the Bio-Rad protein assay.

Semipurification of Cib from *Drosophila* Pupae

All operations were carried out at 4°C. Pupae (30,000) from wild-type or *cib*^{E10} *Drosophila* were crushed and extracted with lysis buffer (25 mM Tris-Cl^{-}, pH 7.8; 1 mM EGTA; 2 mM dithiothreitol; 2 mM 1,2-diaminocyclohexane-N,N,N′,N′-tetraacetic acid; 10% glycerol; 1% Triton X-100; 1 mM PMSF, antiprotease mix). High-speed supernatants (1.7 g protein, 100 ml) were dialyzed overnight against buffer A (20 mM Tris-Cl^{-}, pH 8.0; 1 mM EGTA; 1 mM DTT) and chromatographed on DEAE cellulose (DE-52, Whatman, 2.5 × 30 cm column) equilibrated in buffer A. Following extensive washing with buffer A, a salt gradient from 0 to 0.1 M NaCl in buffer A was applied to the column. Cib (monitored by Western blotting) was eluted at 20–30 mM NaCl. Following fractionated ammonium sulfate precipitation (50%–75% saturation) and dialysis against buffer A, any contaminating profilin was removed by poly-L-proline affinity chromatography. The semipurified preparation was concentrated to 50–60 mg/ml (Centriprep-10, Amicon). The extract from *cib*^{E10} pupae was processed identically. The above steps and the activity assays could be performed in 3 days. Serious difficulties were encountered in trying to improve the purification of Cib due to endemic proteolytic degradation. We failed to absorb Cib on cation exchangers, on G-actin affinity column, and to separate it from a major 23 kDa contaminant by gel filtration.

Antibody Production and Western Blot Analysis

Several dorsal injections of 250 μg of fusion protein GST-Cib mixed with Freund's adjuvant were performed every month for five months in rabbits.

Total proteins of embryos from each stage, third instar larvae, 24-hr-old pupae and adults were isolated by homogenizing frozen animals in a cell culture lysis buffer following instructions from Promega. Fifty micrograms of protein extract was loaded per lane, and Western blots were performed according to Sambrook et al. (1989). Polyclonal antibody against the fusion protein GST-Cib from a single rabbit were used at a 1:8000 dilution.

Central Brain *cib* Expression

cib^{P}*/cib*^{P}*; UAS-mCD8::GFP/+* females were crossed to *UAS-mCD8::GFP/UAS-mCD8::GFP* males. Brains of *cib*^{P}*/+; UAS-mCD8::GFP/UAS-mCD8::GFP* female third instar larvae, 24-hr- and 60-hr-old pupae and adults were dissected and transferred on slides in a drop of PBS. GFP expression was directly checked under a Leica fluorescence microscope.

For whole-mount brain in situ hybridization, an antisense RNA probe labeled with Digoxygenin-UTP encompassing the entire *cib* cDNA of LP07643 clone was obtained by in vitro transcription (Boehringer RNA labeling kit). Brains of *CS* and *cib*^{E10} third instar larvae and 1-day-old pupae were dissected in PBS on ice, transfered in small baskets and fixed 2 hr (1 hr at 4°C, 1 hr at room temperature). All procedures were performed according to Poeck et al. (1993), except that RNase T1 (1 unit/ml) was added to RNase A in RNA digestion step. Signals were analyzed after 210 min in dark conditions.

Analysis of Central Brain Phenotypes

cib^{E10} females were mated to *gal1625,UASmCD8::GFP*. Brains of the offspring males were dissected and GFP expression was analyzed by confocal microscopy.

The overexpression of *cib* was performed using the *hs-cib*$^{+}$ or *UAS-cib*$^{+}$ constructions. *gal623, UASmCD8::GFP* flies were mated with *hs-cib*$^{+}$ or *CS* flies (as a control of the effect of thermic shock on MB development). Heat shock (37°C) was performed for 30 min every 12 hr on eggs of all stages up to imago emergence. *UAS-cib*$^{+}$ flies were crossed to *gal623, UASmCD8::GFP*, or *gal4350,*

UASmCD8::GFP flies. Brains of the offspring were dissected and GFP expression was checked as described.

Heat shock treatment of *cib^{P}/Y; hs-cib^{+}/+* individuals during development did not allow rescue of the adult *cib* defect. Similarly, *cib^{P}/Y; UAS-cib^{+}/+* adults displayed a mutant brain phenotype. The lack of rescue might be due to the fact that fine posttranscriptional regulations normally occur. These could involve the 5′ untranslated sequences absent in the *hs-cib^{+}* and *UAS-cib^{+}* constructs.

Brain Paraffin Sections

Brain sections were performed according to Heisenberg and Böhl (1979). Heads were cut in 7 mm serial frontal sections and inspected under a Leica fluorescence microscope.

Actin Polymerization Measurements

Steady-state measurements of F-actin (critical concentration plots) were derived from fluorescence measurements of pyrenyl-labeled actin (Pantaloni and Carlier, 1993). Actin (10% pyrenyl labeled) as polymerized under physiological ionic conditions (0.1 M KCl, 1 mM $MgCl_2$) in the absence or presence of gelsolin (at 1:300 molar ratio to actin) and in the absence or presence of Cib at the indicated concentrations. The value of the equilibrium dissociation constant for the Cib-actin complex CA was calculated from the measurements of the amount of unassembled actin at steady state [A_u] when barbed ends were capped by gelsolin (Pantaloni and Carlier, 1993) as follows:

$$[A_u] = [A] + [CA]$$
$$[C_{total}] = [C] + [CA]$$
$$[A] = C_c$$
$$K = [C] \bullet [A]/[CA] = ([C_{total}] - [A_u] + C_c) \bullet C_c/([A_u] - C_c)$$

Rates of filament growth from the barbed or pointed ends were measured using either spectrin actin seeds or gelsolin-actin seeds, respectively. Gelsolin-actin seeds were prepared by premixing gelsolin and 2.5 molar equivalent CaATP-G-actin in G buffer. The adequate amount of seeds was added at time zero together with salt to a solution of MgATP-G-actin and Cib.

Analytical Ultracentrifugation

ATP-G-Actin (5 μM) and Cib (5 μM or 10 μM) were mixed in a G buffer and centrifugated in Optima XL (Beckman) at 50,000 × g at 20°C. Scanning was performed at 278 nm.

EDC Cross-Linking of Cib and G-actin

Cib (10 μM) and 5 μM G-actin were mixed in 10 mM sodium phosphate buffer (pH 7.5), 5 mM 1-ethyl-3-(3-dimethylaminopropyl)carbodiimide (EDC), and 5 mM N-hydroxy-succinimide. The solution was incubated on ice for 30 min. Following addition of 10 mM DTT, samples were boiled in SDS/β-mercaptoethanol for 3 min and submitted to SDS–PAGE (Laemmli).

Listeria Motility Assay

The actin-based motility of *Listeria* was reconstituted in vitro from pure proteins as in Loisel et al. (1999). Samples for phase contrast optical microscopy observation were prepared and rate measurements were performed as described (Laurent et al., 1999).

Acknowledgments

We thank Dominique Pantaloni for helpful discussions. We thank Jose Campos-Rifoldi and Michel Chaminade for immunizing rabbits, Dominique Didry for actin purification and labeling and for the purification of proteins used in motility assays, Michèle Dumas for assistance with genetic experiments, and Michel Laurent (Orsay University) for providing advice for confocal analysis. We thank Michael Bubb (University of Florida, Gainsville) for the gift of actobindin and Yukio Doi (University of Kyoto, Japan) for the gift of gelsolin. We thank Kei Ito for sharing unpublished information. We thank BDGP for providing cDNA clones and Kathy Matthews of the Bloomington stock center for providing *Drosophila* strains. We thank Raphael Hitier, Roger Karess, Alberto Pascual, and Florian Petit for providing thoughtful comments on the manuscript. Isabelle Boquet was supported successively by fellowships from the Ligue contre le Cancer (Comité de l'Essonne) and from the Association pour la Recherche contre le Cancer. Rajaa Boujemaa was supported by a fellowship from the Ministère de l'Enseignement Supérieur et de la Recherche. The Association pour la Recherche contre le Cancer (to M.-F. C. and T. P.), the Fondation Pour La Recherche Médicale (to T. P.), the Association Française contre les Myopathies (to M.-F. C.), the Ligue contre le Cancer (comité de l'Essonne [T. P.] and Comité National [M.-F. C.]), and the Human Frontier Science Program (M.-F. C.) provided research financial support.

Received March 10, 2000; revised August 10, 2000.

References

Armstrong, J.D., De Belle, J.S., Wang, Z., and Kaiser, K. (1998). Metamorphosis of the mushroom bodies; large-scale rearrangements of the neural substrates for associative learning and memory in Drosophila. Learning Mem. *5*, 102–114.

Awasaki, T., Saito, M., Sone, M., Suzuki, E., Sakai, R., Ito, K., and Hama, C. (2000). The *Drosophila* trio plays an essential role in patterning of axons by regulating their directional extension. Neuron *26*, 119–131.

Benlali, A., Draskovic, I., Hazelett, D.J., and Treisman, J.E. (2000). *act up* controls actin polymerization to alter cell shape and restrict Hedgehog signaling in the *Drosophila* eye disc. Cell *101*, 271–281.

Boquet, I., Hitier, R., Dumas, M., Chaminade, M., and Preat, T. (2000). Central brain postembryonic development in Drosophila: implication of genes expressed at the interhemispheric junction. J. Neurobiol. *42*, 33–48.

Bradke, F., and Dotti, C.G. (1999). The role of local actin instability in axon formation. Science *283*, 1931–1934.

Brand, A.H., and Perrimon, N. (1993). Targeted gene expression as a mean of altering cell fates and generating dominant phenotypes. Development *118*, 401–415.

Bubb, M.R., and Korn, E.D. (1995). Kinetic model for the inhibition of actin polymerization by actobindin. Biochemistry *34*, 3921–3926.

Bubb, M.R., Lewis, M.S., and Korn, E.D. (1991). The interaction of monomeric actin with two binding sites on Acanthamoeba actobindin. J. Biol. Chem. *266*, 3820–3826.

Carlier, M.F., Laurent, V., Santolini, J., Melki, R., Didry, D., Xia, G.X., Hong, Y., Chua, N.H., and Pantaloni, D. (1997). Actin depolymerizing factor (ADF/cofilin) enhances the rate of filament turnover: implication in actin-based motility. J. Cell Biol. *136*, 1307–1322.

Carlier, M.F., Ducruix, A., and Pantaloni, D. (1999). Signalling to actin: the Cdc42-N-WASP-Arp2/3 connection. Chem. Biol. *6*, 235–240.

Carlier, M.F., and Pantaloni, D. (1994). Actin assembly in response to extracellular signals: role of capping proteins, thymosin beta 4 and profilin. Semin. Cell Biol. *5*, 183–191.

Casella, J.F., Barron-Casella, E.A., and Torres, M.A. (1995). Quantitation of Cap Z in conventional actin preparations and methods for further purification of actin. Cell Motil. Cytoskeleton *30*, 164–170.

Cooley, L., Verheyen, E., and Ayers, K. (1992). chickadee encodes a profilin required for intercellular cytoplasm transport during Drosophila oogenesis. Cell *69*, 173–184.

Crittenden, J.C., Skoulakis, E.M.C., Han, K.A., Kalderon, D., and Davis, R.L. (1998). Tripartite mushroom body architecture revealed by antigenic markers. Learning Mem. *5*, 38–51.

Didry, D., Carlier, M.F., and Pantaloni, D. (1998). Synergy between actin depolymerizing factor/cofilin and profilin in increasing actin filament turnover. J. Biol. Chem. *273*, 25602–25611.

Egile, C., Loisel, T.P., Laurent, V., Li, R., Pantaloni, D., Sansonetti, P.J., and Carlier, M.F. (1999). Activation of the CDC42 effector N-WASP by the Shigella flexneri IcsA protein promotes actin nucleation by Arp2/3 complex and bacterial actin-based motility. J. Cell Biol. *146*, 1319–1332.

Erickson-Viitanen, S., Ruggieri, S., Natalini, P., and Horecker, B.L. (1983). Distribution of thymosin beta 4 in vertebrate classes. Arch Biochem. Biophys. *221*, 570–576.

Gallo, G., and Letourneau, P.C. (1999). Axon guidance: a balance of signals sets axons on the right track. Curr. Biol. *9*, 490–492.

Hanesch, U. (1986). Der zentral complex von *Drosophila melanogaster*. PhD thesis, Bayerischen Julius-Maximilians-Universität Wuerzburg.

Hanesch, U., Fiscbach, K.F., and Heisenberg, M. (1989). Neuronal architecture of the central complex in *Drosophila melanogaster*. Cell Tissue Res. *257*, 343–366.

Hannappel, E., Xu, G.J., Morgan, J., Hempstead, J., and Horecker, B.L. (1982). Thymosin beta 4: a ubiquitous peptide in rat and mouse tissues. Proc. Natl. Acad. Sci. USA *79*, 2172–2175.

Heisenberg, M., and Böhl, K. (1979). Isolation of anatomical brain mutants of *Drosophila melanogaster* by histological means. Z. Naturforsch. B, 143–147.

Ito, K., Awano, W., Suzuki, K., Hiromi, Y., and Yamamoto, D. (1997). The Drosophila mushroom body is a quadruple structure of clonal units each of which contains a virtually identical set of neurones and glial cells. Development *124*, 761–771.

Korey, C.A., and Van Vactor, D. (2000). From the growth cone surface to the cytoskeleton: one journey, many paths. J. Neurobiol. *44*, 184–193.

Kraft, R., Levine, R.B., and Restifo, L.L. (1998). The steroid hormone 20-hydroxyecdysone enhances neurite growth of Drosophila mushroom body neurons isolated during metamorphosis. J. Neurosci. *18*, 8886–8899.

Lanier, L.M., and Gertler, F.B. (2000). From Abl to actin: Abl tyrosine kinase and associated proteins in growth cone motility. Curr. Opin. Neurobiol. *10*, 80–87.

Laurent, V., Loisel, T.P., Harbeck, B., Wehman, A., Grobe, L., Jockusch, B.M., Wehland, J., Gertler, F.B., and Carlier, M.F. (1999). Role of proteins of the Ena/VASP family in actin-based motility of Listeria monocytogenes. J. Cell Biol. *144*, 1245–1258.

Lee, T., Lee, A., and Luo, L. (1999). Development of the Drosophila mushroom bodies: sequential generation of three distinct types of neurons from a neuroblast. Development *126*, 4065–4076.

Lin, M.Z., and Greenberg, M.E. (2000). Orchestral maneuvers in the axon: Trio and the control of axon guidance. Cell *101*, 239–242.

Loisel, T.P., Boujemaa, R., Pantaloni, D., and Carlier, M.F. (1999). Reconstitution of actin-based motility of Listeria and Shigella using pure proteins. Nature *401*, 613–616.

Machesky, L.M., and Insall, R.H. (1999). Signaling to actin dynamics. J. Cell Biol. *146*, 267–272.

Matus, A. (1999). Postsynaptic actin and neuronal plasticity. Curr. Opin. Neurobiol. *9*, 561–565.

Nachmias, V.T. (1993). Small actin-binding proteins: the beta-thymosin family. Curr. Opin. Cell Biol. *5*, 56–62.

Pantaloni, D., and Carlier, M.F. (1993). How profilin promotes actin filament assembly in the presence of thymosin beta 4. Cell *75*, 1007–1014.

Poeck, B., Hofbauer, A., and Pflugfelder, G.O. (1993). Expression of the Drosophila optomotor-blind gene transcript in neuronal and glial cells of the developing nervous system. Development *117*, 1017–1029.

Pollard, T.D., and Cooper, J.A. (1984). Quantitative analysis of the effect of Acanthamoeba profilin on actin filament nucleation and elongation. Biochemistry *23*, 6631–6641.

Pring, M., Weber, A., and Bubb, M.R. (1992). Profilin-actin complexes directly elongate actin filaments at the barbed end. Biochemistry *31*, 1827–1836.

Ramesh, N., Anton, I.M., Hartwig, J.H., and Geha, R.S. (1997). WIP, a protein associated with wiskott-aldrich syndrome protein, induces actin polymerization and redistribution in lymphoid cells. Proc. Natl. Acad. Sci. USA *94*, 14671–14676.

Renn, S.C., Armstrong, J.D., Yang, M., Wang, Z., An, X., Kaiser, K., and Taghert, P.H. (1999). Genetic analysis of the Drosophila ellipsoid body neuropil: organization and development of the central complex. J. Neurobiol. *41*, 189–207.

Ressad, F., Didry, D., Xia, G.X., Hong, Y., Chua, N.H., Pantaloni, D., and Carlier, M.F. (1998). Kinetic analysis of the interaction of actin-depolymerizing factor (ADF)/cofilin with G- and F-actins. Comparison of plant and human ADFs and effect of phosphorylation. J. Biol. Chem. *273*, 20894–20902.

Roth, L.W., Bormann, P., Bonnet, A., and Reinhard, E. (1999). beta-thymosin is required for axonal tract formation in developing zebrafish brain. Development *126*, 1365–1374.

Safer, D., and Chowrashi, P.K. (1997). Beta-thymosins from marine invertebrates: primary structure and interaction with actin. Cell Motil. Cytoskeleton *38*, 163–171.

Sambrook, J., Fritsch, E.F., and Maniatis, T. (1989). Molecular Cloning: A Laboratory Manual, Second Edition (Cold Spring Harbor, NY: Cold Spring Harbor Laboratory Press).

Schneuwly, S., Klemenz, R., and Gehring, W.J. (1987). Redesigning the body plan of Drosophila by ectopic expression of the homoeotic gene Antennapedia. Nature *325*, 816–818.

Simon, A.F., Boquet, I., Synguelakis, M., and Preat, T. (1998). The Drosophila putative kinase linotte (derailed) prevents central brain axons from converging on a newly described interhemispheric ring. Mech. Dev. *76*, 45–55.

Smith, S.J. (1988). Neuronal cytomechanics: the actin-based motility of growth cones. Science *242*, 708–715.

Stossel, V. (1993). On the crawling of animal cells. Science *260*, 1086–1094.

Technau, G., and Heisenberg, M. (1982). Neural reorganisation during metamorphosis of the corpora pedunculata in *Drosophila melanogaster*. Nature *295*, 405–407.

Tettamanti, M., Armstrong, J.D., Endo, K., Yao Yang, M., Furukubo-Tokunaga, K., Kaiser, K., and Reichert, H. (1997). Early development of the Drosophila mushroom bodies, brain centers for associative learning and memory. Dev. Genes Evol. *207*, 242–252.

Truman, J.W. (1990). Metamorphosis of the central nervous system of *Drosophila*. J. Neurobiol. *21*, 1072–1084.

Truman, J.W., Taylor, B.J., and Awad, T.A. (1993). Formation of the adult nervous system. In The Development of *Drosophila melanogaster*, M. Bate and A.M. Arias, eds. (Cold Spring Harbor, NY: Cold Spring Harbor Laboratory Press), pp. 1245–1276.

Vaduva, G., Martin, N.C., and Hopper, A.K. (1997). Actin-binding verprolin is a polarity development protein required for the morphogenesis and function of the yeast actin cytoskeleton. J. Cell Biol. *139*, 1821–1833.

Vaduva, G., Martinez-Quiles, N., Anton, I.M., Martin, N.C., Geha, R.S., Hopper, A.K., and Ramesh, N. (1999). The human WASP-interacting protein, WIP, activates the cell polarity pathway in yeast. J. Biol. Chem. *274*, 17103–17108.

Van Troys, M., Dewitte, D., Goethals, M., Carlier, M.F., Vandekerckhove, J., and Ampe, C. (1996). The actin binding site of thymosin beta 4 mapped by mutational analysis. EMBO J. *15*, 201–210.

Vandekerckhove, J., Van Damme, J., Vancompernolle, K., Bubb, M.R., Lambooy, P.K., and Korn, E.D. (1990). The covalent structure of Acanthamoeba actobindin. Biol. Chem. *265*, 12801–12805.

Verheyen, E., and Cooley, L. (1994). Profilin mutations disrupt multiple actin-dependent processes during Drosophila development. Development *120*, 717–728.

Wills, Z., Marr, L., Zinn, K., Goodman, C.S., and Van Vactor, D. (1999). Profilin and the Abl tyrosine kinase are required for motor axon outgrowth in the Drosophila embryo. Neuron *22*, 291–299.

Yu, F.X., Lin, S.C., Morrison-Bogorad, M., Atkinson, M.A., and Yin, H.L. (1993). Thymosin beta 10 and thymosin beta 4 are both actin monomer sequestering proteins. J. Biol. Chem. *268*, 502–509.